Available online at www.sciencedirect.com

ScienceDirect

Procedia Social and Behavioral Sciences 17 (2011) 438–461

Procedia Social and Behavioral Sciences

19th International Symposium on Transportation and Traffic Theory

Animal dynamics based approach for modeling pedestrian crowd egress under panic conditions

Nirajan Shiwakoti[a]*, Majid Sarvi[a], Geoff Rose[a], Martin Burd[b]

[a]*Institute of Transport Studies, Department of Civil Engineering, Monash University, Melbourne, Victoria, 3800, Australia*
[b]*School of Biological Sciences, Monash University, Melbourne, Victoria 3800*

Abstract

Collective movement is important during emergencies such as natural disasters or terrorist attacks, when rapid egress is essential for escape. The development of quantitative theories and models to explain and predict the collective dynamics of pedestrians has been hindered by the lack of complementary data under emergency conditions. Collective patterns are not restricted to humans, but have been observed in other non-human biological systems. In this study, a mathematical model for crowd panic is derived from collective animal dynamics. The development and validation of the model is supported by data from experiments with panicking Argentine ants (*Linepithema humile*). A first attempt is also made to scale the model parameters for collective pedestrian traffic from those for ant traffic, by employing a scaling concept approach commonly used in biology.

Keywords: Collective patterns, Pedestrians panic, Biological entities, Self-organization, Crowd dynamics, Scaling, Evacuation, Ants, Traffic dynamics

1. Introduction

Collective movement is important during emergencies such as natural disasters or terrorist attacks, when rapid egress is essential for escape. Collective patterns are not restricted to humans, but have been observed in other non-human biological systems. Social animals often move in groups: ant trails, wildebeest migrations, and locust swarms are some of the natural phenomena at the heart of 'movement ecology' (Holden 2006). Although most collective movements are routine, there are rare but perilous crowd panics that may sharply affect survival and fitness, like stampedes of wildebeest under predator attack, evacuations of ant nests in the face of flooding, or flights of people

* Corresponding author. Tel.: +61-3-99051851; fax: +61-3- 9905 4944
E-mail address: nirajan.shiwakoti@monash.edu

1877–0428 © 2011 Published by Elsevier Ltd. Open access under CC BY-NC-ND license.
doi:10.1016/j.sbspro.2011.04.526

from burning buildings. Not enough is known about the underlying dynamics of crowd panics, despite the obvious importance of such knowledge in the human sphere. Studies of human crowds during evacuations were carried out as early as 1930's (Kholshevnikov & Samoshin 2008), but the problem of understanding panicking groups and enhancing safety under emergency conditions still exists (Helbing et al. 2000). The complex interactions of panicking individuals with their social and physical environments make theoretical understanding difficult. Models of pedestrian behavior in emergency situations rarely have complementary empirical data to validate the model's prediction, so we may not want to rely entirely on mathematical models before scaling up to an applied, real world situation. That lack of data is most likely a major factor explaining why very few models exist which focus on panic situations. The bulk of the literature is restricted to the study of normal (non-panic) pedestrian dynamics or normal evacuation processes (Still 2000, Hoogendoorn & Bovy 2002, Hoogendoorn 2004, Daamen 2004, Antonini et al. 2006, Kretz 2007, Asano 2009). Even the researchers who developed the few existing models of crowd panic have identified the need for more rigorous modeling frameworks and the development of approaches to assess the reliability of model predictions (Helbing et al. 2000).

Mathematical simulation models have been used since the 1970's to study the collective movements of animals (Okubo 1986). However, findings from such work are seldom applied to the study of collective human dynamics (Shiwakoti et al. 2009, 2010). Shiwakoti et al. (2009, 2010) highlighted the potential contribution that research with non-human organisms could make to the understanding of complex pedestrian behavior and the enhancement of pedestrian safety during emergency egress. Non-human model organisms differ in many details from humans, but they are at least living creatures and are more life-like than equations. They may be expected to behave and interact in more complex manners. In this paper, a mathematical modeling framework derived from animal dynamics is proposed for the study of crowd panic.

The paper is structured as follows. The next section details the formulation of the proposed model. The development and validation of the model is supported by data from experiments with panicking Argentine ants (*Linepithema humile*). The validation of the developed model is presented next by applying the model to simulate the collective dynamics of panicking ants. The same model is then scaled up for collective pedestrian traffic based on the scaling concept derived from biology. The final section presents the conclusions and recommendations for future research.

2. Model formulation

2.1. Background

Like in vehicular traffic, there are microscopic, mesoscopic and macroscopic modeling approaches for pedestrian dynamics (Shiwakoti et al. 2008). This section is dedicated to the development of a microscopic model for collective pedestrian traffic under panic conditions. The microscopic approach considers the interactions between individuals and may enable better estimates of delays to pedestrians, an aspect of the dynamics that is particularly important in emergency / panic situations. The proposed model is based on observations from experiments with ants, previous studies on animal dynamics, and collective pedestrian dynamics. The model is required to simulate collective traffic across a size gap as large as ants and pedestrians. Therefore, for consistency, non-human organisms or pedestrians are referred to as 'individuals' throughout the model development. The pedestrian crowd is treated as an 'emergent system' for model formulation. Emergent systems, also referred to as self-organized systems, arise from 'The emergence of order on a global scale through interactions on a local scale' (Charlotte 2005). Such order has been observed in flocks, herds, schools, etc., where entities with limited intelligence interact locally, which in turn leads to the emergence of group behavior on a global scale (Charlotte 2005). The simplicity of such interactions in various biological entities has motivated the development of the model in this research on the assumption that pedestrian crowds act as an emergent system. Figure 1 represents the interdependence between individual goals, interactions among individuals, and the emergent group behavior. How pedestrian crowds escape under emergency conditions is highly dependent on how the group goals and individual goals are constituted and coordinated in those situations.

The basic philosophy is to address the complexity of human behavior by assigning each individual (having limited information) with simple locomotion rules as those observed from collective animal dynamics, and observing the emergent group behavior based on the local interactions of the individuals.

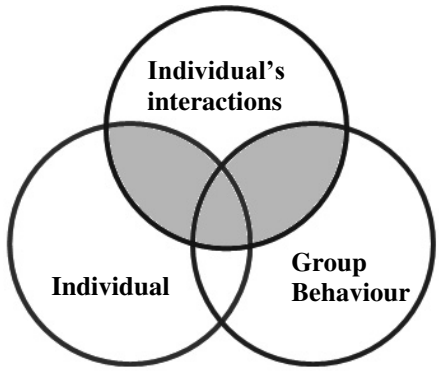

Figure 1 Interdependence between the individual, interactions among individuals, and emergent group behavior

2.2. Modeling platform

Previous studies on collective animal dynamics (Okubo 1986) and limited studies on human panic (Helbing et al. 2000) have been based on Newton's law of Motion. Hence it can be assumed that Newtonian mechanics can be a platform for modeling collective dynamics. Newtonian mechanics state that a temporal change of the momentum of an individual occurs in the direction of the net force which is the product of mass and acceleration as shown below by Equation 1 and 2

$$m_\alpha \, \vec{a}_\alpha = \vec{F} \qquad (1)$$

$$m_\alpha \frac{d^2 x}{dt^2} = \vec{F} \qquad (2)$$

Where,

m_α = mass,

$\vec{a}_\alpha$ = acceleration,

$\vec{F}$ = force.

The acceleration of an individual who is acted on by forces from other individuals and from obstacles and walls would therefore be

$$\vec{a}_\alpha = \frac{1}{m_\alpha}\left(\sum_{\beta=1(\alpha\neq\beta)}^{N} (\vec{F}_{\alpha\beta}) + \sum_{1}^{N_w} \vec{F}_{w\alpha} \right) \qquad (3)$$

Where,

N = number of individuals,

$\vec{F}_{\alpha\beta}$ = forces acting on an individual (α) from another individual (β),

$\vec{F}_{w\alpha}$ = forces acting from surrounding environment such as obstacles and walls,

N_w = number of obstacles and walls.

Based on the acceleration specified in Equation 3, the motion of an individual is uniquely determined as the position and velocity of each individual could be updated in each time step from the integration of the Newton's equation of motion as shown below by Equation 4 and 5.

$$\vec{x}(t+\Delta t) = \vec{x}(t) + \vec{v}(t)\Delta t + \frac{1}{2}\vec{a}(t)\Delta t^2 \quad (4)$$

$$\vec{v}(t+\Delta t) = \vec{v}(t) + \frac{1}{2}\left[\vec{a}(t) + \vec{a}(t+\Delta t)\right]\Delta t \quad (5)$$

Where,

$\vec{x}(t)$, $\vec{v}(t)$ and $\vec{a}(t)$ = position, velocity and acceleration of an individual at time t ,

Δt = time step.

The most important issue here is to identify and represent those collective forces that would be able to produce the collective dynamics of the individuals under panic situations. To understand the nature of these forces, real data of human panic under emergency conditions are required. Such data are rare, however. Hence experiments with Argentine ants were conducted to gain insight into human panic. The next section describes experiments on panicking Argentine ants and the development of an approach to model those collective forces that are analogous to human panic.

2.3. Experiments with panicking ants

2.3.1. Justification on the use of ants

Ant-inspired solutions to crowding problems might be especially useful, in that humans have been dealing with traffic congestion for only a few thousands years at most, while ants have been dealing with congestion over millions of years of evolution. Any common features of dynamical behavior of ants and human pedestrians could make ant colonies a potentially valuable resource for testing models of panic behavior and designs to ameliorate crowd disasters (Burd 2006, Burd et al. 2010). Nishinari et al. (2006) state that there are similarities between ants on a trail and pedestrians in evacuations, since both try to follow the signals of other individuals (through pheromone on a trail and information from one's eyes and ears, respectively). Ants offer a number of advantages compared to other organisms for the study of crowd panic, including their ready availability, ease of handling, and the simplicity of the equipment needed to perform the experiments. Also they are social organisms (Hölldobler & Wilson 1990), which makes them generally comparable to humans. Likewise, there are many species of ants (Hölldobler & Wilson 1990) that may enable researchers to conduct studies around specific properties that a species may possess. One may be skeptical, however, when comparing ants to humans. There are large taxonomic differences that should not be ignored. Also, ants are generally believed to be non-selfish in nature (Hölldobler & Wilson 1990). However, new research suggests that ant society has corruption and cheating similar to human society and that they are not always non-selfish (Hughes and Boomsma 2008). Bourke & Franks (1995) mention that both co-operation and conflicts exists in ant society. Altshuler et al. (2005) suggested that some features of the collective behavior of humans and ants can be quite similar when escaping under panic, despite sizable differences between traffic in humans and ants in normal conditions.

Argentine ants (*Linepithema humile*) have been selected as test organisms in this study. One of the advantages of using Argentine ants is that these species are reported to display natural evacuation process (LeBrun et al. 2007).

These ants are native to the Río Paran´a drainage of subtropical South America (Wild, 2004), where flooding regularly forces colonies to evacuate their nests and seek refuge in trees (LeBrun et al., 2007). In areas where Argentine ants have been introduced, colonies seem to abandon nests frequently (Heller & Gordon, 2006), suggesting that the dynamics of departure from a nest may have large effects on colony fitness.

2.3.2. Experiments

To gain insight into human panic, a series of experiments were performed with Argentine ants under panic conditions. The main motivations for conducting the experiments were to observe and study how collective movement patterns are affected by the layout of the escape area or the presence of certain geometrical structures in the escaping area. These experiments reflect an original attempt to study the effect of structural features to the collective movement patterns of non-human entities during rapid egress and translate those results to the study of human panic. Four scenarios of experimental trials were conducted:

- Ants escaping from a circular chamber without partial obstruction near exit (30 repetitions).
- Ants escaping from a circular chamber with partial obstruction (via a column) near exit (30 repetitions)
- Ants escaping from a square chamber with exit at the middle of the wall (10 repetitions)
- Ants escaping from a square chamber with exit at the corner of the walls (10 repetitions)

Figure 2 shows the schematic diagram of the experimental setup for the square chamber experiments, with an exit located at the corner of the walls or at the middle of the wall, as well as for the circular chamber experiments.

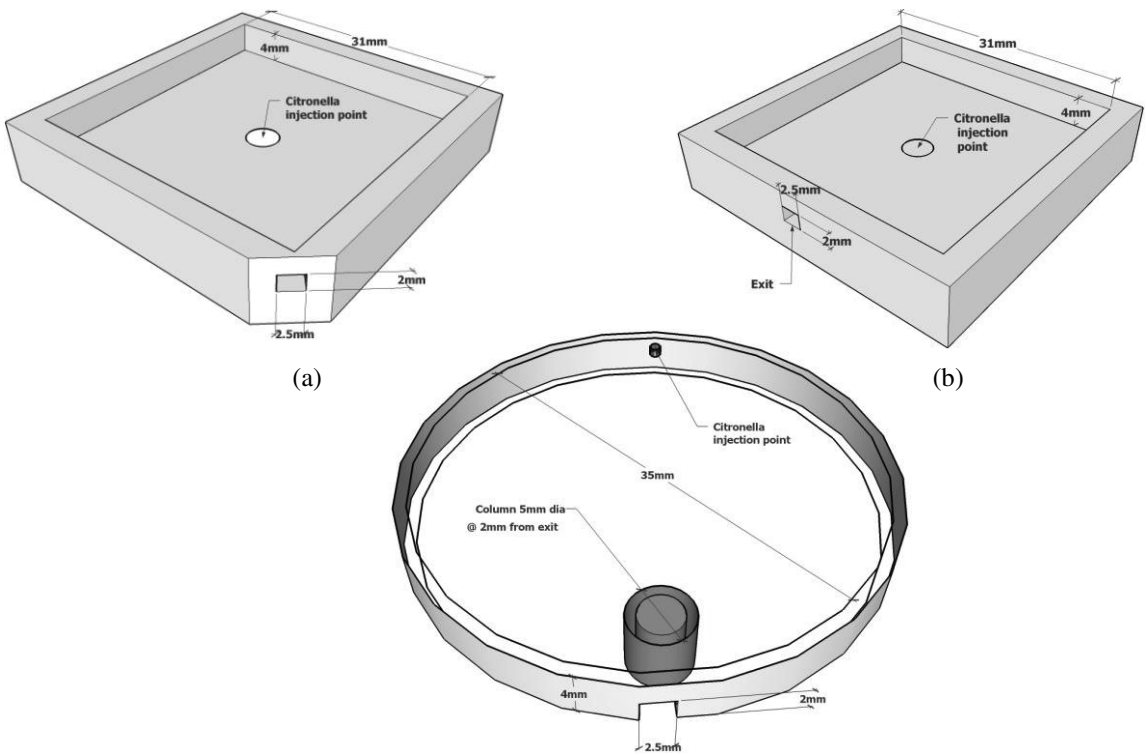

Figure 2 Schematic diagram of experimental setup for exit located at the corner of the walls (a), exit located at the middle of the wall (b) and circular chamber with column (c)

To perform the experiments, the ants (numbering 200-250 in each chamber) were allowed to nest naturally in an evacuation chamber by creating favorable humid conditions. For the circular evacuation chamber, the nest was made from an upturned transparent plastic petri dish lid, 35 mm in diameter and 4 mm deep. Each nest had a single “pin

hole" entrance/exit that was 2.5 mm wide and 2.0 mm high. These dimensions allowed unimpeded passage of a single ant into or out of the nest, or somewhat encumbered passage of two ants simultaneously. To study the effect of a partial obstruction to the exit, a circular plastic column 5 mm in diameter and 4 mm tall was placed 2 mm in front of the exit, slightly asymmetrically to the main axis of the exit. The square chamber experiments employed wooden chambers measuring 31mm by 31mm (the equivalent area to that of circular chambers). The exit width and height were the same as in the circular chamber experiment. The square chambers were covered with transparent Fluon coated plastic 'ceilings' to allow escape only through the single experimental exit. A small hole was created in the chamber ceiling to allow injection of 10 micro-liters of citronella (an insect repellent liquid) for creating panic.

2.3.2.1. Results

Ants rushed toward the exit when the citronella was introduced, in a manner reminiscent of humans in a crowd panic. Figure 3 shows a snapshot of the experiments with corner vs. middle exits on square chambers and the presence or absence of partial obstructions at the exit in circular chambers.

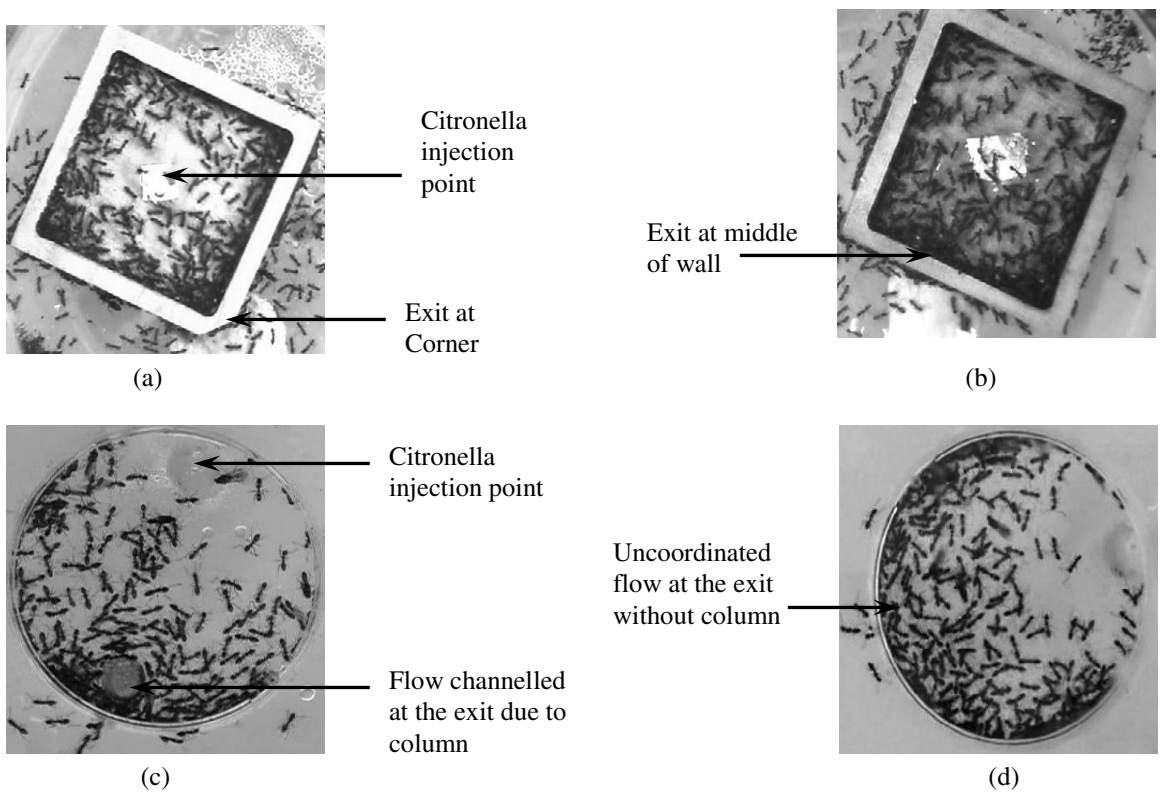

Figure 3 Snapshots of the experiment with panicking ants: exit located at the corner (a), exit located at the middle of wall (b), column near exit (c) and without column near exit (d)

When panic was created, the density of ants became quite elevated near the nest exit, resulting in frequent contacts. However, they tried to avoid colliding with each other when they were very close (<1mm) or when contact actually occurred. Thus, the ants had restricted movement near the exit. Further back, where inter-individual distances were 1mm to approximately 8mm inter-individual distance, the density was not as high and the mobility of ants was not as constrained as near to the exit. Beyond 8mm from their nearest neighbor, the ants were attracted to the exit on a random basis. The existence of these different zones can be conceptualized as the zone of attraction and

repulsion, similar to what has been observed in the collective dynamics of schools and flocks (Okubo 1986). Thus, it is observed from the experiments that the repulsion zone existed at a distance less than 1mm while attraction zone existed after 1mm and up to approximately 8 mm. From the video data of the experiments, evacuation time (to the nearest second) and number of ants that escaped was measured by manual counting from playback of digital video recordings.

In the experiments with a square chamber, mean escape time for 50 ants (based on first and second cohort of 50 ants) was 12.9 seconds when the exit was at the corner and 20.4 seconds when the exit was at the middle of a wall, an approximately 58% faster evacuation when the exit was located at the corner. Figure 4 shows the comparison of the mean escape time for different cohort of ants (first or second group of 50 ants) for exit at the middle of the wall and at the corner. Escape times in both treatments were lower for the first 50 ants than for the next 50. Escape was always faster with the exit at the corner. The results from a repeated measures ANOVA test are shown in Table 1. There were highly significant differences in evacuation times between trials with the corner and centre exit as revealed by F-value and P-value ($F_{1, 18} = 21.85$, $P < 0.001$, Table 1). The main effect of the corner exit is significant. Cohorts differed significantly in their escape time and there was no exit × cohort interaction (Table 1, Figure 4).

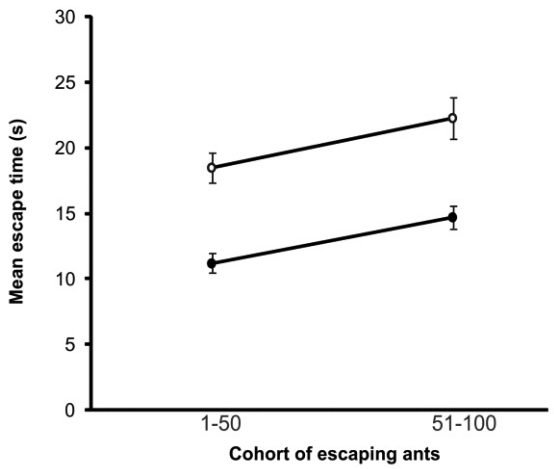

Figure 4 Mean escape times for the first and second cohorts of 50 ants to leave the nest under panic conditions. Open symbols indicate the exit located at the centre and closed symbols indicate the exit located at the corner. Error bars show ±1 SE (standard error).

Table 1 ANOVA results for the effect of exit at corner / middle and cohort sequence on escape time

Effect	Degree of Freedom (df)	Mean-Square	*F-value*	*P-value*
Between-subjects				
(Exit at corner / middle)	1	551.75	21.85	<0.001
Error	18	25.25		
Within-subjects repeated measure				
(1st, 2nd cohort)	1	133.66	20.97	<0.001
Cohort × Exit treatment	1	0.19	0.03	0.87
Error	18	6.38		

One reason for this reduction in evacuation time at a corner exit could be the minimization of directional changes by escaping ants. With a centre exit, ants escaping along both sides of the wall had to change their direction at the exit in order to evacuate. That resulted in interactions with the ants that were moving straight towards the exit. In the corner exit, the ants escaping from the side walls near the corner could pass through without much change in their original direction. This result suggests the role that change in direction among individual members in a crowd (during collective dynamics) may play in facilitating or hindering the escape of a crowd.

From the experiments in a circular chamber, mean escape time for 50 ants (based on two cohorts of 50 escaped ants) was 14.0 seconds when the column was present and 20.1 seconds when it was not, i.e., about 44% slower under the ostensibly more favorable conditions of an unobstructed exit. Figure 5 shows the comparison of mean escape time for different cohort of ants in trials with/without a column. The effect of a column near the exit was statistically significant, as revealed from a repeated measures ANOVA test with p-value <0.001. The presence of a column in front of the exit channeled the traffic in a manner that did not occur with an unimpeded exit. One manifestation of this channeling was that lone exits (a single individual passing through the exit hole rather than temporal overlap of two or more individuals) were more common when the column was present. Of the first 50 ants to escape in each trial, an average of 24.1 ($\pm$ 5.3 standard deviation) were lone exits when the column was present and 19.1 ($\pm$ 4.4 standard deviation) when it was absent as revealed by the P-value from the t-test ($t_{16} = 2.17$, $P = 0.022$, one tailed test). The net effect was that the flux of ants through the exit was improved, on average, by the presence of the partial obstruction. This increase in the flow due to obstruction near the exit is consistent with mathematical predictions for pedestrian crowds (Helbing et al. 2002). This result demonstrates the large role seemingly small structural features can play during collective movements.

The empirical data and observations from the above experiments suggest the nature of the collective forces that are to be modelled in the following sections. These data also provide various testing and validation scenarios for the prediction model to be developed. Empirical experiments of this kind might compensate for the scarcity of data on human panics, and provide reassurance that a model correctly identifies the essential features of solutions that are efficacious and improve the safety of pedestrians.

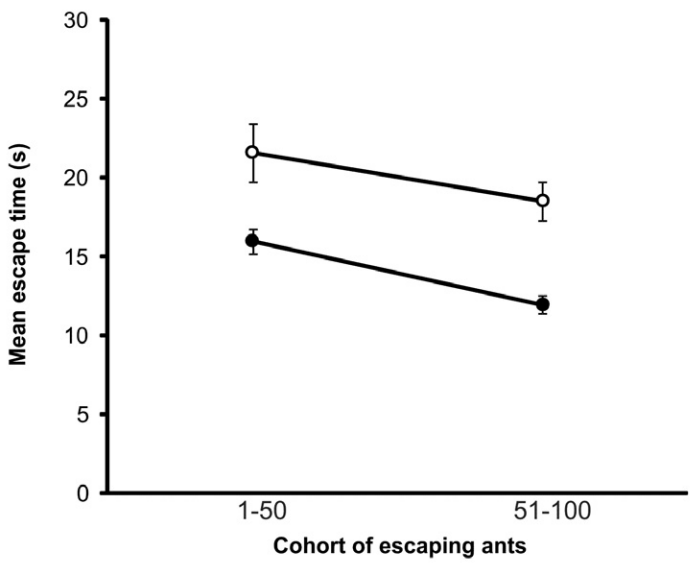

Figure 5 Mean escape times for the first and second cohorts of 50 ants to leave the nest under panic conditions. Open symbols indicate the absence of a column as a partial exit obstruction and closed symbols indicate presence of a column. Error bars show ±1 SE.

2.4. Modeling collective forces

In the ants experiment, it was observed that their movement in response to certain stimuli (here citronella) does not necessarily follow a simple set of rules. As in animal dynamics, there were predictable responses, such as taxis (a term the biological literature uses) where an animal displays guided movement towards or away a stimulus. As citronella was repellent to ants, they showed negative taxis, moving away from the stimulus towards the exit. This is similar to what one can expect when a crowd of people is running away from source of danger (e.g., a fire) towards a safe place. However, in some cases, there were movements so irregular they can be regarded as a random motion, especially in the attraction zone (1mm-8mm inter-individual distance) and beyond (>8mm inter-individual distance). Examples of random motion such as klinokinesis, which involves change in the frequency and direction of movement in response to the stimulus, or orthokinesis, in which the speed of movement is altered, could be observed in the ants experiment. These movements are similar to those observed in animal dynamics (Okubo 1980). However, it has been observed that even kinesis is not entirely random and that the degree of response depends on the strength of the stimulus, so that the motion appears to be deterministic in a statistical sense (Okubo 1980). One can expect similar kinds of taxis and kinesis during collective dynamics of pedestrian crowds as well. Thus, when considering crowd dynamics, it is necessary to divide the forces acting on an individual into random and non-random components. These forces, as detailed in the following sections, underlie the detailed development of the modeling framework.

2.4.1. Non-random forces

2.4.1.1. Impulsive forces

In the experiment, panic among ants is associated with increase in fleeing speed from 3mm/s (normal) to 9mm/s (panic). This phenomenon of increase in fleeing or desired speed is also observed in other non-human organisms such as schools of fish and flocks of birds, when exposed to frightening stimuli (Okubo 1986). An increase in desired speed (of up to 5-10m/s) has also been associated with panic in pedestrian crowds (Helbing et al. 2000). This increase in fleeing speed and running towards a safe place/exit could be viewed as the combination of positive orthokinesis, negative klinokinesis and positive taxis which result a strong tendency to aggregate toward the source of the stimulus (here safe exit). The acceleration resulting from these impulsive forces could be thus modelled as proportional to their fleeing speed as shown below:

$$\vec{a}_I \propto v_f \frac{\vec{d}(t) - \vec{p}_\alpha(t)}{\left\| \vec{d}(t) - \vec{p}_\alpha(t) \right\|} \tag{6}$$

Where,

$\vec{a}_I$ = impulsive acceleration

v_f = fleeing speed

$\frac{\vec{d}(t) - \vec{p}_\alpha(t)}{\left\| \vec{d}(t) - \vec{p}_\alpha(t) \right\|}$ = unit vector from a particular position of an individual $\vec{p}_\alpha(t)$ towards exit $\vec{d}(t)$ at the characteristic time (t)

For accelerative equilibrium of impulsive forces and resistive forces, a constant, termed the relaxation time (σ^{-1}) needs to be included. In particular, the use of relaxation time (σ^{-1}) is valid when the resistance force is linearly proportional to the velocity (Okubo 1980). Hence Equation 6 can be written as

$$\vec{a}_I = \sigma^{-1} v_f \frac{\vec{d}(t) - \vec{p}_\alpha(t)}{\left\| \vec{d}(t) - \vec{p}_\alpha(t) \right\|} \quad (7)$$

2.4.1.2. Local interactive forces

Individuals have limited information and vision during emergency conditions (collective motion); i.e., they consider only the things that they can see in their immediate surroundings. Thus local interactions are important. In the ants experiments, there was evidence of formation of attraction and repulsion zones (which were a function of the inter-individual distance). The existence of these different zones is similar to that observed in the collective dynamics of schools, flocks and swarms. For example, the critical distance that fish in schools maintain from each other varies within 16 to 25% of their mean body length, while attractions start at a distance beyond their body length (Okubo 1986). Okubo (1980), reports that during insect swarming, the interior of the swarm consists of a number of sub-swarms moving in random directions. However, the insects at the leading, peripheral and rear edges show a consistent orientation toward the interior of the swarm enabling them to migrate for many hours without disrupting its coherence. Okubo (1986) mentions that a wave of agitation propagated through schools of fish exposed to frightening stimuli in an experiment. The formation of "shock waves" was due to a rapidly shifting zone in which the fish reacted to the actions of their neighbors by changing their own positions. The speed of the wave's propagation reached 11 to 15 m/s, which is much higher than the maximum forward speed of individual fish (about 1 m/s). Similarly, when predators attacked bird flocks, formation of a "ball" of birds has been observed along with an increase in their flight speed. At times, the flock "pulsated" (expanding and contracting in a spatial sense) as inter-bird distance varied (Okubo 1986). Kholshevnikov & Samoshin (2008) reviewed studies on pedestrian evacuation carried out by researchers in Russia and elsewhere in the world and identified identical structures of collective pedestrian flow. They mention that the distance between people constantly changes and causes local squeezing which later on disappears and then appears again. Such "pulsating" collective dynamics behavior is similar in schools, flocks and swarms as explained above.

Assuming that individuals during panicking situations have limited information and vision (due to high crowd density and short time for egress), there appears to be striking similarities in the structure and behavioral rules of the collective dynamics of several biological organisms, such as schools, swarms, flocks, and also human groups. These similarities are vital for maintaining the coherence of the collective dynamics. These behavioral rules, as observed from the ants experiments and in animal dynamics (Okubo 1980, Matuda & Sannomiya 1985), can be represented conceptually as a relationship between interpersonal distance and the resulting repulsive and attractive forces. It is proposed that the regulation of collective patterns of individual dynamics to perceived risk results directly from a change in interaction range, i.e. the attraction and repulsion range as represented in Figure 6. The repulsive forces depend on the proximity of individuals. The magnitude of the repulsive forces is large when interpersonal distance is small, and decrease with increasing distance until a point where the interpersonal distance exceeds the repulsion range. At that point, attractive forces begin to act on pedestrians to draw them together, until the maximum point of attraction is reached. At even greater separation, the attractive forces would start decreasing and eventually have a negligible effect. While the concept of repulsive forces based on interpersonal distance has been addressed previously (Helbing et al 2000, Hoogendoorn 2002, Hoogendoorn 2004), the importance of attractive forces has received limited attention in the study of the collective pedestrian motion. The "pulsating" nature of the collective movements of pedestrian crowd in panic situation can only be captured correctly if both attractive and repulsive forces are considered.

The non-linear local interactive forces (both attractive and repulsive), as discussed above and represented conceptually in Figure 6, need to be mathematically represented and included in the model. Inspired from behavioral rules in animal dynamics (Okubo 1980, Matuda & Sannomiya 1985), here it is assumed that local interactive forces are inversely proportional to the square of the distance between individuals, similar to Newton's law of gravitation, and given by

$$\vec{F}_L = \phi\ W(\theta_{\alpha\beta})\left(\frac{\left[\left(X_{\alpha\beta} - r_{\alpha\beta}\right) - \lambda_R\right]}{\left[\left(X_{\alpha\beta} - r_{\alpha\beta}\right) - \lambda_R\right]^2 + \lambda_A^2}\right)\vec{n}_{\alpha\beta} \quad (8)$$

$\phi = \phi_R$ When $\left(X_{\alpha\beta} - r_{\alpha\beta}\right) < \lambda_R$ (repulsive forces)

$\phi = \phi_A$ When $\left(X_{\alpha\beta} - r_{\alpha\beta}\right) > \lambda_R$ (attractive forces)

Where,

$\vec{F}_L$ = local interactive forces (repulsive and attractive),

ϕ =constant,

$X_{\alpha\beta}$ = interpersonal distance between individuals (centre to centre),

$r_{\alpha\beta} = r_\alpha + r_\beta$ =sum of radii of the circular representation of the individuals,

λ_R = repulsion distance,

λ_A = attraction distance,

$\vec{n}_{\alpha\beta}$ = normal unit vector,

$W(\theta_{\alpha\beta})$ = a weighing factor

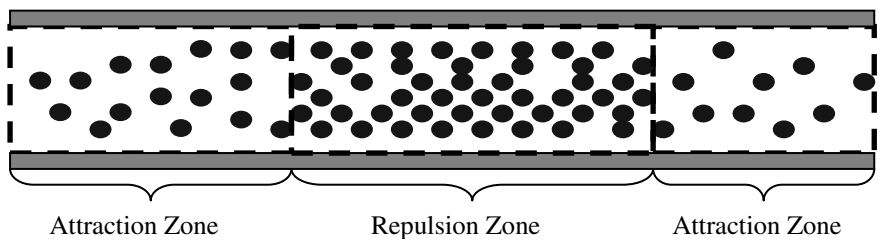

(a)

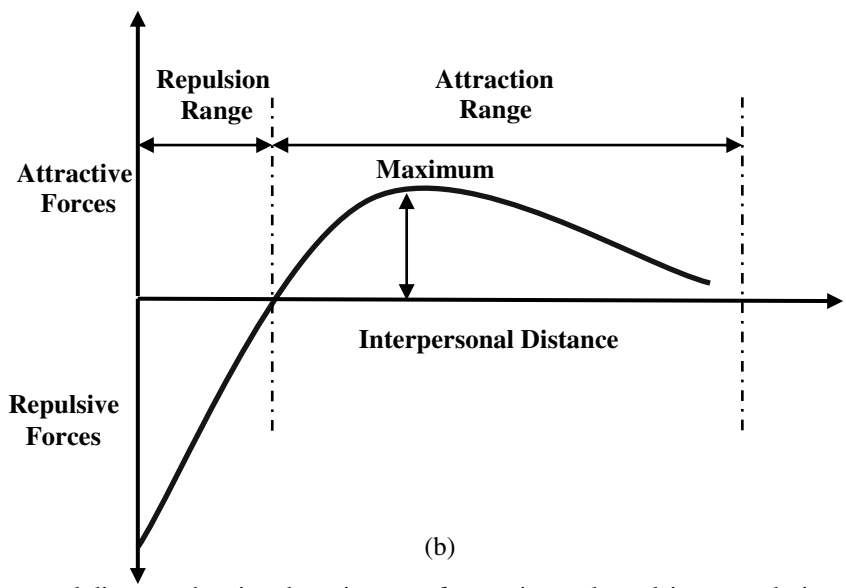

(b)

Figure 6 Conceptual diagram showing the existence of attractive and repulsive zone during collective dynamics (a) and nature of repulsive and attractive forces based on interactive range of interpersonal distance (b)

The variation in repulsive and attractive forces is achieved by introducing different constants ϕ_R and ϕ_A for repulsive and attractive forces, respectively, to tune the model for collective traffic. It is important to consider the anisotropic factors for pedestrian behaviour (Hoogendoorn & Bovy 2002, Hoogendoorn & Daamen 2007). For that, a weighing factor $W(\theta_{\alpha\beta})$ that represents the influence of the individual in front and back has been included in Equation 8 based on the angle between individuals ($\theta_{\alpha\beta}$). Figure 7 (a) shows the components of the interactive forces as described above while Figure 7(b) shows how the weighing factor varies as a function of the angle $\theta_{\alpha\beta}$. The function $W(\theta_{\alpha\beta})$ is given by

$$W(\theta_{\alpha\beta}) = 1 - \left(\frac{1 - \cos\theta_{\alpha\beta}}{2} \right)^2 \qquad (9)$$

The weighing factor is maximum when the individual (β) is in front of individual (α), and decreases as the position of individual (β) shifts to the side or behind individual (α).

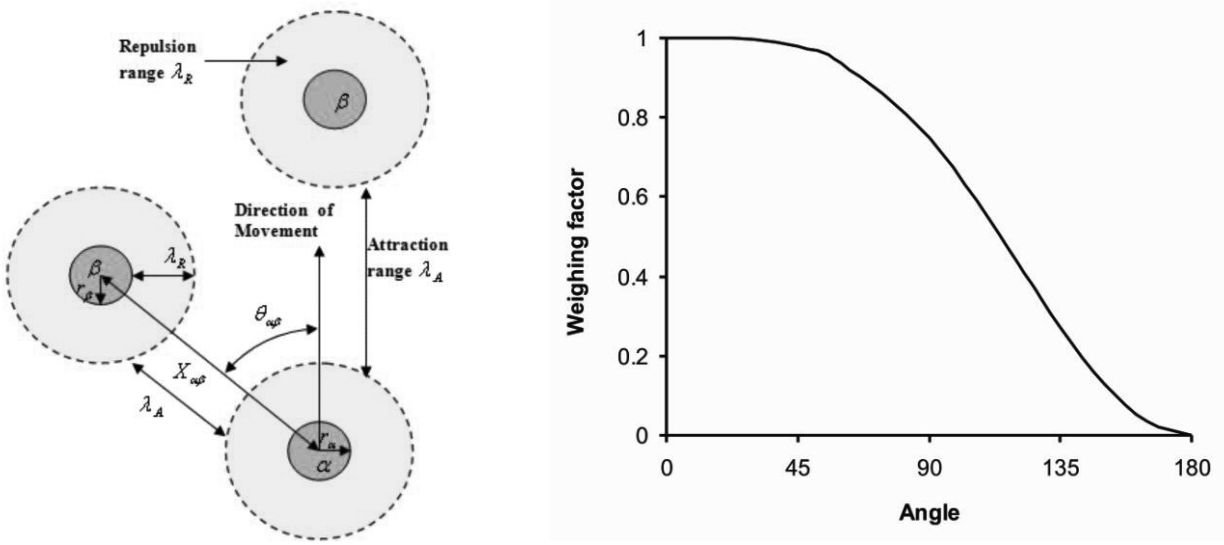

(a) (b)

Figure 7 Schematic diagram showing components of local interactive forces (a) and variation of the weighing factor as the function of the angle between two individuals (b)

2.4.1.3. Collision and pushing forces

As observed from the experiments, the density of ants became elevated near the exit. When ants were moving at high speed towards the exit, frequent collisions with mutual interactions occurred near the exit. At high density or high speed, individuals tend to come very close and sometimes push each other. In such instances, there is the possibility that individuals collide or overlap each other in the simulation. Likewise, consideration of the pushing forces is necessary to take into account additional delays incurred due to such mutual interactions. In these cases, repulsive forces alone are not enough. These collisions and overlapping phenomena also have been a notable problem in the study of rigid spherical body collisions in molecular dynamics (Rapport 1995). The problem is usually addressed by incorporating strong normal forces as well as frictional (shearing) forces between the colliding particles in order to avoid overlapping. An analogous approach can be taken for particle-based simulation of

collective traffic. As shown in Figure 8, the initial velocity (dashed arrow) gets diverted to a new direction due to a normal force and a shear force. The normal and shear forces acting on two colliding particle can be modeled by Equation 10 and 11 as mentioned in Cundall & Strack (1979), Bell (2005).

$$\vec{F}_n = \alpha_1 \varepsilon^{\delta} \vec{v}_m + \alpha_2 \varepsilon^{\varphi}\, \vec{n} \quad (10)$$

$$\vec{F}_t = \mu_1 \vec{v}_t \quad (11)$$

Where,

$\vec{F}_n$ = normal force

$\vec{F}_t$ = shear force

$\vec{v}_m$ = relative velocity in normal direction

ε = overlap

δ, φ = constant

α_1 = damping coefficient controlling dissipation during collisions

α_2 =elastic restoration coefficient controlling particle stiffness

$\vec{v}_t$ =relative velocity in shearing direction

μ_1 = friction coefficient

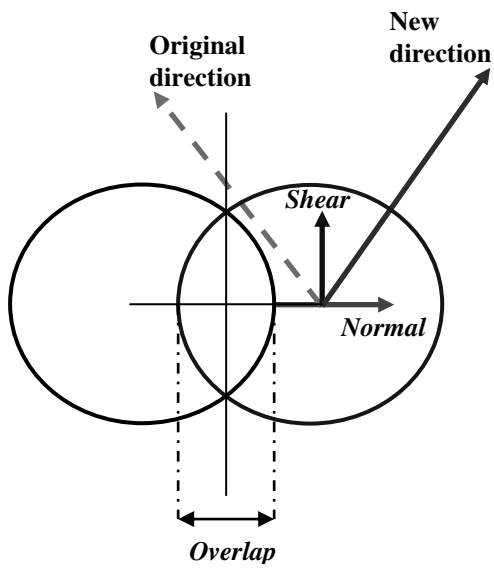

Figure 8 Components of pushing forces to avoid collision based on inelastic sphere collision concept of molecular dynamics

In the simplest case, one can choose δ =0 and φ =1 and obtain a damped linear spring force. Thus equation 10 and 11 can be modified to represent the pushing forces as below

$$\vec{F}_n = \alpha_1 \vec{v}_m + \alpha_2 \varepsilon\, \vec{n} \quad (12)$$

$$\vec{F}_t = \mu_1 \vec{v}_t + \mu_2 \varepsilon\, \vec{t} \quad (13)$$

$$\vec{F}_P = \vec{F}_n + \vec{F}_t = \alpha_1 \vec{v}_m + \alpha_2 \varepsilon\, \vec{n} + \mu_1 \vec{v}_t + \mu_2 \varepsilon\, \vec{t} \quad (14)$$

Where,

$\vec{F}_P$ = pushing force

μ_2 = friction coefficient

$\vec{t}$ =unit vector in shearing direction

An expression similar to those for local interactive forces and collision/ pushing holds true for interactive forces from stationary obstacles such as walls and columns as specified in Equation 3. Here $\alpha_1, \alpha_2, \mu_1$ and μ_2 can be chosen to match experimental data or manually tuned to produce the desired response. Helbing et al. (2000) proposed a similar approach for modeling pushing forces, however there are some differences between Helbing's approach and that reflected in Equations 12 and 13 in this paper, primarily due to the addition of terms $\alpha_1 \vec{v}_m$ and $\mu_2 \varepsilon \vec{t}$ in Equations 12 and 13 respectively. The extra term $\alpha_1 \vec{v}_m$ is added in Equation 12 to take into account the effect of relative velocity in normal direction as well. Also the term $\mu_2 \varepsilon \vec{t}$ considered in Equation 13 can accommodate the case of relative velocity at or near zero. In the absence of term $\mu_2 \varepsilon \vec{t}$, the frictional force would be zero if relative velocity is near or equal to zero, and that may cause instability in the simulation if the desired speed is high.

2.4.2. Randomness

As discussed earlier, one can expect randomness in the behavior of individuals during panic situations. The disturbances produced due to such random behavior could be the result of several factors and thus could be a function of differences in mass, speed, size, cognitive abilities, and other biological traits of the individuals. That is

$$\vec{\xi} = f \text{ (mass, } \textit{speed, size, cognitive abilities, psychological state.....)} \quad (15)$$

Where,

$\vec{\xi}$ = fluctuations arising from randomness

In the following section, this random component, reflecting individual heterogeneity, is included in the equation for instantaneous acceleration.

2.4.3. Operation of the model

With the collective forces modeled as described in section 2.4, the optimal instantaneous acceleration of the individual as mentioned in Equation 3 can now be written as

$$\vec{a}_\alpha = \vec{a}_I + \frac{1}{m_\alpha}\left[\sum_{\beta=1(\alpha\neq\beta)}^{N} \vec{F}_{\alpha\beta} + \sum_{1}^{N_w} \vec{F}_{w\alpha}\right] + \vec{\xi} \quad (16)$$

Or,

$$\vec{a}_\alpha = \vec{a}_I + \frac{1}{m_\alpha}\left[\sum_{\beta=1(\alpha\neq\beta)}^{N} (\vec{F}_L + \vec{F}_P) + \sum_{1}^{N_w} \vec{F}_{w\alpha}\right] + \vec{\xi} \quad (17)$$

It is difficult to solve Equation 17 analytically; hence simulation is the preferred approach. The instantaneous acceleration specified in this equation can be updated in each small discrete time step based on the integration of the equations of motion as previously stated in section 2.2. As the model formulated is a continuous one, the time step for the update needs to be very small to minimize the error due to assignment of discrete time steps for a continuous model.

2.5. Scaling model parameters

One can take into account the difference in magnitude of the parameters in ant traffic and pedestrian traffic through 'scaling effects'. That is to say, if one organism was built to the same design as another, but on a different scale, the various characteristics of the original would necessarily be scaled up or down to produce a working model. A power formula is usually used in biology to describe the relationship (often termed an *allometric relation*) between an animal's body mass (M) and another of its characteristics (C) (Peters 1999) i.e.

$$C = k_1 M^k \tag{18}$$

Where k_1 and k are constants

The change of C with respect to M is called the scaling of that characteristic to body size. These allometric equations are usually transformed to logarithms to linearize the relation and make it simpler to draw and interpret the change of C at different values of M as shown in following equations

$$\log C = \log(k_1 M^k) \tag{19}$$

$$\log C = \log k_1 + k \log M \tag{20}$$

In biology, many aspects of locomotion follow similar power laws with respect to body mass, even across a size gap as large as ants to humans. Maximum velocity commonly follows a power-law scaling with respect to body size for each locomotory mode of swimming, running and flying (Peters 1999). Consistent with the intuition, larger animals usually run faster than smaller ones, and maximum speed increases with size. The scatter of data, however, allows exceptions for particular comparisons (e.g. a cheetah can run faster than an elephant). However, the overall pattern shows a positive scaling relation between maximum speed $(V_{\max})$ and body size (*M*) given by (Peters 1999)

$$V_{\max} \propto M^{0.38} \tag{21}$$

Given an average mass of 70 kg for a pedestrian and 4.8×10^{-4} gm for an Argentine ant, a pedestrian is 1.5×10^{8} heavier than an Argentine ant. Bursts of speed over short distances in human crowd panics can reach 5–10 m/s as noted in Section 2.4.1.1. A scaling exponent of 0.38 applied to an average human pedestrian and Argentine mass implies that panic speed of the ants should reach 4–8 mm·s^{-1}. From the experimental measurements, the average speeds of Argentine ants changed from 3 to 9 mm·s^{-1} when transitioning from normal activity to induced panic. That suggests it is reasonable to accept 0.38-power scaling for the human-ant comparison. Therefore, for scaling model parameters, simple proportional scaling of the model parameters based on the body mass difference between humans and ants has been considered by using Equation 21. Hence, the scaling factor (S) for model parameters is proportional to $M^{0.38}$ i.e.

$$S \propto M^{0.38} \tag{22}$$

Or,

$$S = \psi M^{0.38} \tag{23}$$

Where,
ψ = constant

3. Validation of model

In this section, the simulation model proposed above is validated for simulation of ant traffic and pedestrian traffic. For ant traffic, first the model is calibrated for scenarios with and without a column being present near the exit and then the model is validated with independent data from scenarios with an exit at the corner or the middle of a wall as explained in section 2.3. The model must be appropriately parameterized for ant traffic before scaling up to the human situation. Following that scaling, the model is applied to simulate collective pedestrian egress for the experimental scenarios as described for ant traffic. The performance of the model is also validated through a comparison of the flow rate of pedestrian through a bottleneck, measured experimentally under non-panic condition.

3.1. Simulation of ant traffic

In calibrating the model, some of the parameter values were measured and obtained from the experiment (such as desired speed, mass, size, reaction time, repulsion and attraction range). Because of the difficulty in directly measuring the other parameters (such as repulsive and attractive force constants, dampening and elastic restoration constant, frictional constant), those parameters were estimated from simulation trials so as to replicate the experimental scenario. A local sensitivity analysis was performed to gain insight into how the simulation output changes when one or more parameters are changed. The parameters value were estimated based on their relatively stability for 5% changes in the model parameters. The values of the parameters used for the simulation are given in Table 2. A total of 200 ants were distributed randomly at the start of each simulation. The time step (Δt) for the update of the simulation was 0.001s. For simplicity, the representation of the effective area occupied by ants has been considered with an equivalent circular representation as has been used for modeling pedestrians based on circular particles analogy (Helbing et al. 2000). The more rigorous representation like a rectangle can be adopted in future. However, in this study, it is assumed that the analogy of circular representation is adequate, as the primary aim of this manuscript is about understanding the minimum underlying mechanisms of self-driven particles in crowds despite variations in biological idiosyncrasies. Even in simulation of human panic, it has been suggested that consideration of non-circular shaped pedestrian bodies has minimal effect on escape (Helbing et al. 2000) although research are being undertaken to study the influence on dynamics due to other shapes such as elliptical ones (Chraibi et al. 2010).

Table 2 Value of the parameters assessed for the simulation of escape rate of ants

From experimental measurement		From estimation	
Parameters	Value	Parameters	Value
v_f	9 mm/s	ϕ_R	0.1 g mm2 / s2
σ	0.2s	ϕ_A	2.5*10-4 g mm2 / s2
m_α	3.4*10-4 g to 6.2*10-4 g	α_1	0.01 g/s
r_α , r_β	0.5 mm to 0.6 mm	α_2	8 g/ s2
λ_R	0.5 mm	μ_1	0.06 g/s
λ_A	8.0 mm	μ_2	0.06 g/ s2

In the experiment, with an unobstructed exit, evacuation times for the first 50 ants ranged from 10.76 to 48.20s (mean ± s.d = 21.6 s ± 9.9 s), while in the presence of a column, evacuation times ranged from 9.00 to 25.66 s (mean

± s.d = 16.0 s ± 4.3 s). The corresponding results for the simulations were 14.41 to 27.42 s (mean ± s.d. = 18.9 s ± 2.6 s) without the column, and 11.5 to 21.86 s (mean ± s.d = 13.9 s ± 1.9 s) with the column present. Figure 9 shows the typical curve obtained from the simulation for scenarios with and without the column being present. From Figure 9, it can be seen that the difference in evacuation time with and without the column increases as time elapses and the cumulative number of evacuated ants increases. This may occur because there will be more frequent strong local interactions as more individuals gather at the exit. The presence of a column helps to minimize the number of interactions and thereby avoiding the delay in egress. If such strong local interactions slow people by even a few seconds, or a fraction of a second, during emergency egress, the delay could influence their chance of survival.

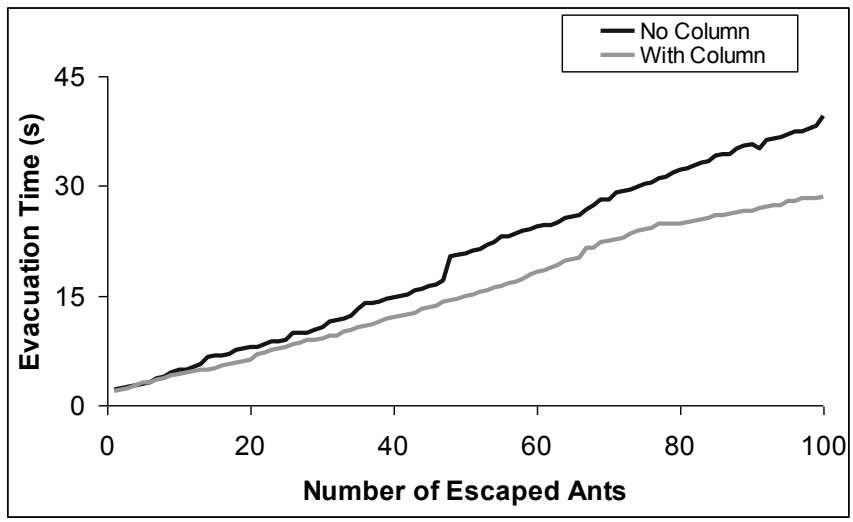

Figure 9 Comparison of typical ant escape rate curve from simulation trials for with and without column scenario

Table 3 shows the headway distributions classified into three classes: gaps up to 0.5 s in length, gaps greater than 0.5 s up to 1 s, and gaps greater than 1s. Again results are shown for scenarios with/without column and for both empirical and simulation data. Differences between the outcomes with and without a column present near the exit are statistically significant for both the empirical and simulation data as shown by Chi-squared test ($\chi^2 = 37.4$, $P < 0.001$ for empirical data and $\chi^2 = 122.6$, $P << 0.001$ for simulation data). Chi-squared values (degree of freedom = 2), test the homogeneity of frequencies in the results for scenarios with/without the column. The proportion of headways less than or equal to 0.5 s is higher in the case of the column present near the exit (80.7% in the experiment and 92.4% in the simulation) compared to the case of the column being absent (71.3% in the experiment and 78.6 % in the simulation). In contrast, the proportion of headways greater than 0.5 s is higher in the case when the column is absent (20.5% in the experiment and 15.4 % in the simulation) compared to the case when the column is present (14.9 % in the experiment and 6.7% in the simulation). These results suggest that with the column located near the exit, the frequency of long time headways decreases while there is an increase in the frequency of short headways thereby facilitating the rapid succession of exits compared to the case when there is no column near the exit.

The model predicted that the corner exit is more efficient for facilitating the egress of ants compared to the exit located at the middle of wall. With a corner exit, experimental evacuation times for the first 50 ants ranged from 8.24 to 14.84 s (mean ± s.d = 11.18 s ± 2.61 s), while for the case of the middle exit, evacuation times ranged from 12.0 to 27.64 s (mean ± s.d = 18.48 s ± 4.09 s). The corresponding results for the simulations were 11.83 to 15.27s (mean ± s.d = 12.98 s ± 1.11 s) with the corner exit, and 14.41 to 24.69 s (mean ± s.d = 19.02 s ± 2.89 s) with the middle exit. Table 4 consolidates the headway distributions into three classes: gaps up to 0.5 s in length, gaps greater

than 0.5 s up to 1 s, and gaps greater than 1 s. Differences between the outcomes with the exit located at the corner and middle of the walls are statistically significant for both the empirical and simulation data as shown by Chi-squared Test ($\chi^2 = 44.24$, $P < 0.001$ for empirical data and $\chi^2 = 31.74$, $P < 0.001$ for simulation data). As in the case where the column was introduced near an exit, it is the reduction of longer headways and an increase in shorter headways that makes the corner exit more efficient compared to the exit located at the middle of a wall.

Table 3 Frequency of headways in the empirical and simulation data (column vs. no column)

	Empirical data		Simulation data	
Headway interval, t (s)	Column present	Column absent	Column present	Column absent
$t \leq 0.5$	80.7%	71.3%	92.4%	78.6%
$0.5 < t \leq 1$	14.9%	20.5%	6.7%	15.4%
$t > 1$	4.4%	8.2%	0.9%	6.0%

Table 4 Frequency of headways in the empirical and simulation data (corner vs. middle exit)

	Empirical data		Simulation data	
Headway interval, t (s)	Corner exit	Middle exit	Corner exit	Middle exit
$t \leq 0.5$	91.4%	76.5%	90%	77.2%
$0.5 < t \leq 1$	8%	18.2%	8.6%	6.9%
$t > 1$	0.6%	5.3%	1.4%	5.9%

3.2. Simulation of pedestrian traffic

Following the successful calibration and validation of the model for ant traffic in Section 3.1, this section examines the performance of the model when it is scaled up to simulate collective dynamics of pedestrians. The motive for this was to test the robustness of the model with respect to differences in the size, speed, and other biological details of the panicking individuals. There is scope within such a test to compare the collective movement patterns of biological entities and pedestrians in order to devise sound strategies to aid evacuation. The model was used to study pedestrian traffic for panic conditions as well as for normal (non-panic evacuation) conditions. For panic conditions, the model was validated with the experimental scenarios as described for ant traffic but scaled up for the human scenario. For normal (non-panic) conditions, the model was validated with experimental data on pedestrian traffic; specifically the comparison of outflow in bottlenecks with various widths. Parameter values in the model were either taken from the available empirical data on pedestrian traffic (e.g. mass, size, speed) or *allometrically* scaled up from the ant values based on the body mass difference (as explained in Section 2.5) where direct measurement of parameter values was not possible.

3.2.1. Non-panic escape

The ability of the model to replicate non-panic conditions was assessed based on the comparison of the simulation results with those of experimental data for flow at a bottleneck under normal conditions. The bottleneck experiments were conducted by researchers at the University of Duisburg-Essen, Germany (Kretz 2007). The experiments involved a unidirectional movement of 100 pedestrians (3 trials each) passing through a bottleneck of various widths; 80 cm, 100 cm and 120 cm respectively.

The bottleneck was formed by two cabinets with a height of two meters and a depth of 40 centimeters. The pedestrians were confined in an area approximately 9 m deep and 4m wide. The pedestrian movement through

bottleneck was recorded by a video camera mounted above the bottleneck. As the simulation was for normal conditions, the frictional / pushing forces were not considered i.e. μ_1 and $\mu_2 = 0$. Also the desired speed was assigned to be 1m/s corresponding to the free velocities for leaving a room under normal conditions (Helbing et al. 2000).

Figure 10 shows a snapshot from the experiment and the corresponding simulation. Figure 11 compares the flow as obtained from the simulation with that from the experiment for the various bottleneck widths. As observed in experiment, the model is sensitive to changes in egress width which result in corresponding changes in exit flow rates. The model also predicted flow rates through the bottleneck which corresponded closely to the values measured in the experiment (Figure 11).

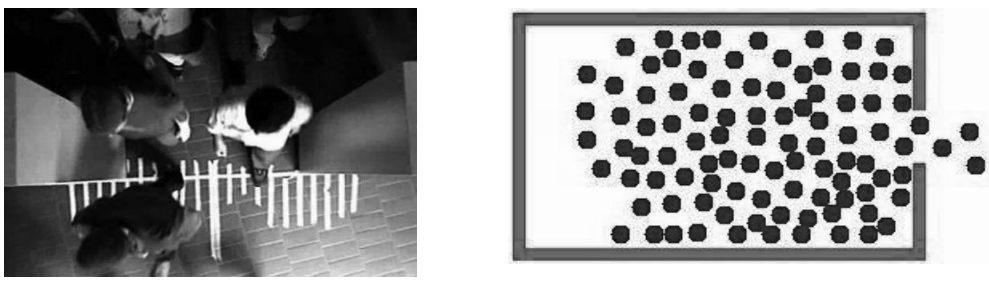

(a) (b)

Figure 10 Snapshots showing the experimental setup for bottleneck experiments (a) and corresponding simulation setup (b)

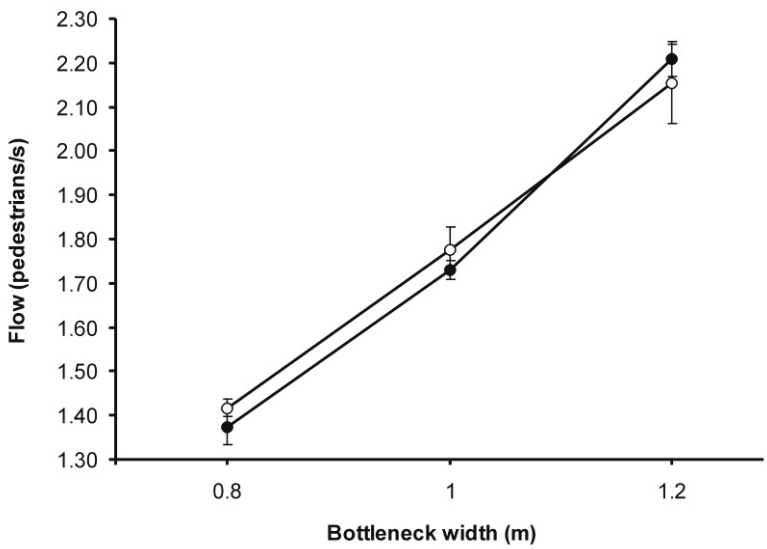

Figure 11 Comparison of flow through bottleneck of various widths from simulation to those observed from experiment. Error bars show ±1 SE. Open symbols, empirical results; filled symbols, model results. Error bars show ± 1 S.E.

3.2.2. Panic escape

Mirroring the scenarios considered in the ants experiments, simulation of pedestrians under panic were considered for cases with/without a column near the exit of a room and for exits located at the corner and centre of the room. Two hundred pedestrians were distributed randomly in a room 15m by 15m in size and were allowed to escape through a single door with a width of 1.2m. For the column trial, a 1.5 diameter column was placed slightly asymmetrically near the exit at a distance of 0.5 m from the exit. The desired velocity of 5m/s corresponded to the fleeing velocity under panic conditions reported in the literature (Helbing et al. 2000). Randomness or some arbitrary irregularities in the simulation was introduced via a distribution of different body sizes, masses and influence of individuals to the front and back of a focal individual. The parameters for the simulation were scaled up from ant traffic based on the scaling concept derived in section 2.5. Consistent with the experiments from panicking ants, the simulation model predicted an increase in the evacuation rate of the pedestrians with the column near the exit compared to when the column was absent. The model also predicted that corner exit is more efficient compared to the exit located at the middle of the wall. Figure 12 presents simulation snapshots for those scenarios. Figures 13 and 14 compare the flow based on 10 simulation trials for column/no column and centre exit/middle exit scenarios.

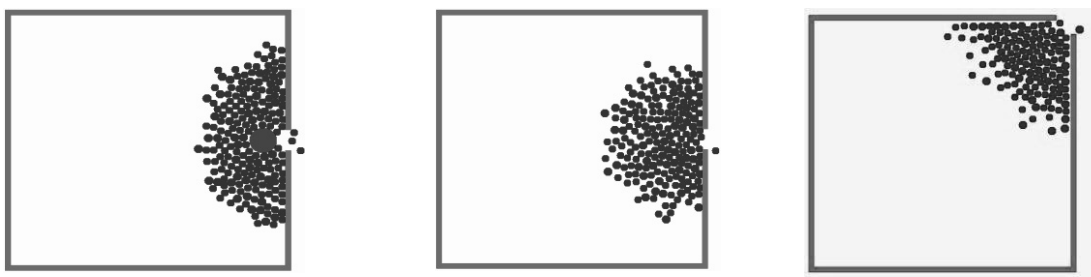

(a) (b) (c)

Figure 12: Simulation snapshots showing panicked pedestrian escaping from a room with partial obstruction (via column) near the exit (a), without obstruction (b) and the exit located at the corner (c)

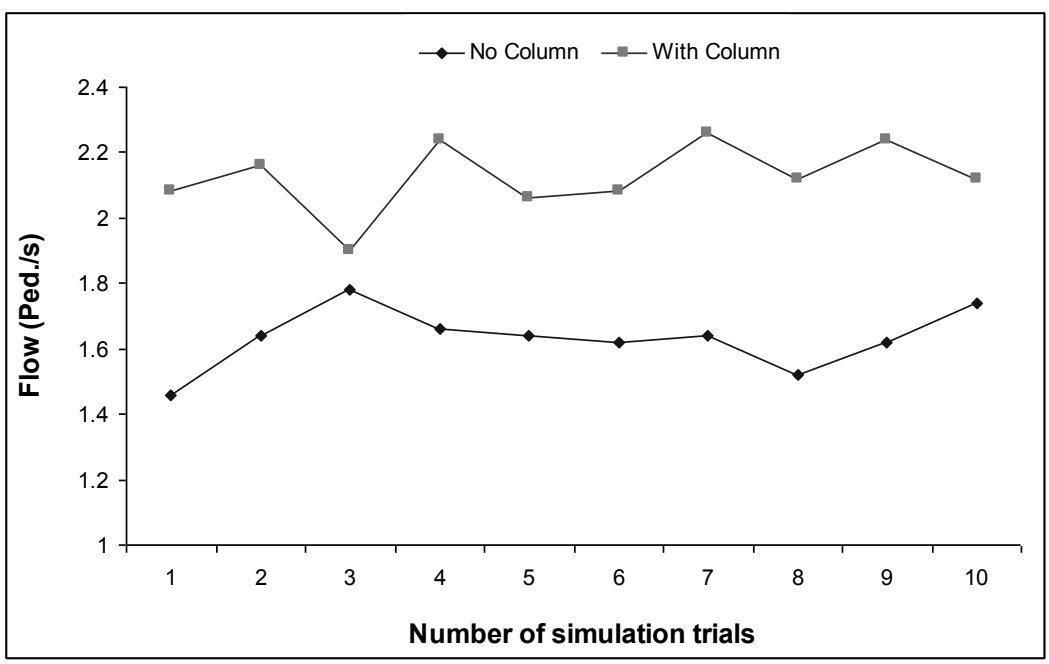

Figure 13 Comparison of flow for with/without column scenario from simulation

It can be seen from Figure 13 that the presence of partial obstruction such as column near the exit generally increases the exit flow. The average flow was 1.63 ped./s without the column while it was 2.12 ped./s when the column was present. Thus the presence of the column increased the efficiency of escape by 30%. It is also interesting to compare the flow through a 1.2 m bottleneck from the experiment (2.15 ped./s, Figure 11) to that from the simulation for panic conditions (1.63 ped./s, Figure 13 with no column scenario). It can be observed that as expected, the flow under panic conditions is much less (32%) than under non-panic condition for the same bottleneck width of 1.2m. Likewise from Figure 14, it can be seen that corner exit improves the flow of the people compared to middle exit. The average flow was 3.01 ped./s with the corner exit compared to 1.63 ped./s with the middle exit.

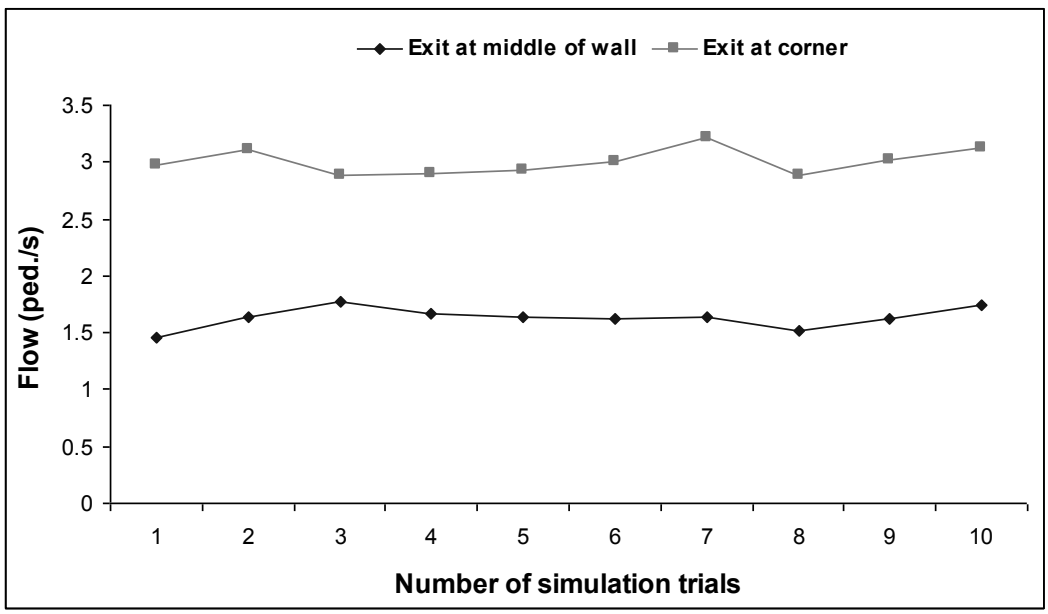

Figure 14 Comparison of flow for exit at corner / middle scenario from simulation

4. Conclusions

This paper has demonstrated a methodology of using non-human organisms in the development of a pedestrian traffic model under panic conditions through an innovative approach which integrates biology and traffic engineering. The contributions from this manuscript are:

- The experiments reported in this study reflect an original attempt to study the effects of structural features or the layout of the escape area on the collective movement patterns of non-human entities during rapid egress and to translate those results to the study of human panic. Most importantly, it has demonstrated how such empirical data from non-human organisms such as ants can overcome the shortage of human panic data for model calibration and validation, something which has intrigued researchers for decades. The experiments that are reported here also addresses gaps in the study of alarm traffic in social insects, by drawing attention to the relationship between nest architecture and internal traffic under alarm conditions. The model organism approach is commonplace in medical research but not in engineering, yet we believe it has enormous potential in providing insight and theoretical understanding of crowd panic. It will help us understand what properties of panic are inherent to the physical nature of crowds, and what properties depend on the idiosyncratic details.
- An additional advance in terms of modeling is the consideration of both attractive and repulsive forces under panic condition to maintain the coherence of collective dynamics. The consideration of repulsive forces

existed in the literature on human panic, but to our knowledge there was no consideration of the role of attractive forces. We applied the concepts of an attraction zone and a repulsion zone from collective animal dynamics (and also as observed in our experiments with ants) to the collective dynamics of pedestrians. We have also modified the frictional forces (based on molecular dynamics) as used in previous models of panic to consider the difficulties in the stability of the simulation (especially at high desired speed) when the relative velocity of an individual is near or equal to zero.

- Employing a scaling concept derived from biology reflects an innovative approach to scale the model parameters with respect to body mass difference across a size gap from ants to humans. We know of no other research which has attempted to apply this concept to human panic. The lack of data on panic has presented challenges for researchers in developing confidence in the values chosen for parameters, particularly when those parameter values are usually arbitrarily chosen. However, in our approach, we scaled up the parameters for humans from ants and thus the value of parameters in our model has a defensible foundation. With this framework, there is scope to compare the collective movement patterns of non-human biological entities and pedestrians in order to devise sound strategies to aid evacuation.

The proposed model provides insight into the minimal interactions or physical mechanisms required for the emergence of collective dynamics and the nature of those underlying mechanisms through experiments with panicking ants. The effectiveness of the proposed modeling framework was validated through simulation of panicking ant traffic as observed from the experiment and then scaling up for human situations. The simulation results show consistency with the observed data from the experiment. Successful prediction of collective movement in both humans and Argentine ants in our study demonstrates that the model captures something fundamental about the dynamics of self-driven particles in crowds despite variation in size, manner of locomotion, cognitive abilities, and other biological traits. The capability of the developed model to accommodate both non-panic and panic conditions within the same modeling framework for pedestrian crowds was also demonstrated. As research on crowd panic is a continuously challenging process, future research can continue to explore how insight from other fields, such as biological science, can help develop the capability to model the behavior of pedestrian crowds under panic conditions. It is possible that in the future we may see more algorithms, design solutions and models of pedestrian traffic with contributions from the study of social insects and other social animals.

Acknowledgements

The authors would like to thank Dr. Tobias Kretz, PTV AG, Software Development Traffic Engineering, Germany for providing the experimental data relating to pedestrian traffic through a bottleneck.

5. References

Altshuler, E., Ramos, O., Núñez, Y., Fernández, J., Batista-Leyva, A.J. and Noda, C. (2005). Symmetry breaking in escaping ants. *The American Naturalist*, 166 , pp. 643–649

Antonini, G., Bierlaire, M., and Weber, M. (2006). Discrete choice models of pedestrian walking behavior. *Transportation Research Part B*, 40, issue 8, pp. 667-687

Asano, M., Kuwahara, M. and Tanaka, S. (2009). A pedestrian theory considering anticipatory behaviour for capacity evaluation. In W.H.K Lam, S.C Wong & H.K. Lo (Eds.), *Transportation and traffic flow theory* (pp. 559-582), Springer

Bell, N., Yu, Y. and Mucha, J.P. (2005). Particle-based simulation of granular materials. Proceedings of the ACM SIGGRAPH/Eurographics Symposium on Computer Animation, ACM New York, pp.77-86

Bourke, F.G. A. and Franks, R.N. (1995). *Social evolution in ants*. Princeton University Press

Burd, M. (2006). Ecological consequences of traffic organization in ant societies. *Physica A,* 372, pp. 124 -131

Burd, M., Shiwakoti, N., Sarvi, M. and Rose, G. (2010). Nest architecture and traffic flow: large potential effects from small structural features. *Ecological Entomology*, 35, issue 4, pp. 464-468

Charlotte, K.H. (2005). *Self-organization and evolution of social systems*. Cambridge University Press

Chraibi, M., Seyfried, A. and Schadschneider, A. (2010). Generalized centrifugal force model for pedestrian dynamics. Physical Review E 82, pp. 046111 (1-9).

Cundall, P.A., and Strack, O.D.L (1979). A discrete numerical model for granular assemblies. *Geotechnique*, 29, pp. 47-65

Daamen, W. (2004). *Modelling passenger flows in public transport facilities* (Doctoral *dissertation*, Delft University of Technology, 2004). Retrieved from http://repository.tudelft.nl/

Helbing, D., Farkas, I. and Vicsek, T. (2000). Simulating dynamical features of escape panic. *Nature*, 407, pp. 487-490

Helbing, D., Farkas, I.J., Molnar, P. and Vicsek, T. (2002). Simulation of pedestrian crowds in normal and evacuation situations. In M. Schreckenberg & S. D. Sharma (Eds.), *Pedestrian and Evacuation Dynamics (pp.21-58)*, Springer Berlin

Heller, N.E. and Gordon, D.M. (2006). Seasonal spatial dynamics and causes of nest movement in colonies of the invasive Argentine ant (*Linepithema humile*). *Ecological Entomology*, 31, 499–510

Holden, C. (2006). Inching toward movement ecology. *Science*, 313, 779–782

Hölldobler, B. and Wilson O.E. (1990). *The Ants*. The Belknap Press of Harvard University Press, Cambridge, Massachusetts.

Hoogendoorn, S.P. and Bovy, P.H.L. (2002). Normative Pedestrian Behaviour Theory and Modelling. In M. Taylor (Eds.), *Transportation and traffic flow theory in the 21st century* (pp.219-246), Elsevier

Hoogendoorn, S.P. (2004). Pedestrian flow modeling by adaptive control. In *Transportation Research Record: Journal of the Transportation Research Board*, *No. 1878*, Transportation Research Board of National Academies, Washington, D.C., pp. 95–103

Hoogendoorn, S. P. and Daamen, W. (2007). Microscopic calibration and validation of pedestrian models: cross-comparison of models using experimental data. In A. Schadschneider, T. Pöschel, R. Kühne, M. Schreckenberg & D.E. Wolf (Eds.), *Traffic and granular flow '05*, pp. 329-340, Berlin, Heidelberg: Springer

Hughes, O. H.W. and Boomsma, J.J. (2008). Genetic royal cheats in leaf-cutting ant societies. *Proceedings of the National Academy of Sciences (PNAS),* 105, no. 13, pp. 5150–5153

Kholshevnikov, V.V. and Samoshin, D.A. (2008). Laws of motion of pedestrian flow-Basics for evacuation modelling and management. In H.J Pasman & I.A. Kirillov (Eds.), *Resilience of cities to terrorist and other threats* (pp. 417-442), Springer Science

Kretz, T. (2007). *Pedestrian traffic: simulation and experiments* (Doctoral dissertation, University of Duisburg-Essen, 2007). Retrieved from http://www.d-nb.de/eng/index.htm

LeBrun, E.G., Tillberg, C.V., Suarez, A.V., Folgarait, P.J., Smith, C.R. and Holway, D.A. (2007). An experimental study of competition between fire ants and Argentine ants in their native range. *Ecology*, 88, 63–75

Matuda, K. and Sannomiya, N. (1985). Computer Simulation of Fish Behaviour in Relation to a Trap Model. *Bulletin of the Japanese Society of Scientific Fisheries*, 51(1), pp. 33-39

Nishinari, K., Sugawara K., Kazama, T., Schadschneider, A. and Chowdhury, D. (2006). Modelling of self-driven particles: Foraging ants and pedestrians. *Physica A*, 372, pp. 132-141

Okubo, A. (1980). *Diffusion and ecological problems: Mathematical models*. Springer-Verlag, Germany

Okubo, A. (1986). Dynamical aspects of animal grouping: swarms, schools, flocks and herds. *Adv. Biophys*., 22, pp 1-94

Peters, H.R. (1999). *The ecological implications of body size.* Cambridge University press.

Rapport, C.D. (1995). *The art of molecular dynamics simulation*. Cambridge University Press

Shiwakoti N., Sarvi, M. and Rose, G. (2008). Modelling pedestrian behaviour under emergency conditions – State-of-the-art and future directions. Australasian Transport Research Forum (ATRF), Australia, 31, pp. 457-473

Shiwakoti N., Sarvi, M., Rose, G. and Burd, M. (2009). Enhancing the safety of pedestrians during emergency egress: Can we learn from biological entities? *Transportation Research Record,* No. 2137, pp. 31-37.

Shiwakoti N., Sarvi, M., Rose, G. and Burd, M. (2010). Biologically inspired modeling approach for collective pedestrian dynamics under emergency conditions. *Transportation Research Record*, No. 2196, pp. 176-184

Still, G. K. (2000). *Crowd Dynamics* (Doctoral dissertation, University of Warwick, 2000). Retrieved from http://www.gkstill.com/PhDThesis.html

Wild, A.L. (2004). Taxonomy and distribution of the Argentine ant, *Linepithema humile* (Hymenoptera: Formicidae). *Annals of the Entomological Society of America*, 97, 1204–1215